17th World Conference on Earthquake Engineering, 17WCEE
Sendai, Japan - September 13th to 18th 2020

Design of a Tuned Mass Damper Inerter using optimization based on exhaustive search for the vibration control of a seismically excited structure

L. Lara[(1)], D. Caicedo[(2)], Y. Farbiarz[(3)], J. Brito[(4)], Y Valencia[(5)]

[(1)] *Associate Professor, Universidad Nacional de Colombia, Facultad de Minas, Sede Medellín, Departamento de Ingeniería Civil, A.A. 75267, Medellín, Colombia, lualarava@unal.edu.co*
[(2)] *Master Student, Universidad Nacional de Colombia, Facultad de Minas, Sede Medellín, Departamento de Ingeniería Civil, A.A. 75267, Medellín, Colombia, dcaicedod@unal.edu.co*
[(3)] *Professor, Universidad Nacional de Colombia, Facultad de Minas, Sede Medellín, Departamento de Ingeniería Civil, A.A. 75267, Medellín, Colombia, jfarbiar@unal.edu.co*
[(4)] *Associate Professor, Department of Civil and Environmental Engineering Universidade de Brasilia (Brazil), jlbrito@unb.br*
[(5)] *Associate Professor, Universidad Nacional de Colombia, Facultad de Minas, Sede Medellín, Departamento de Ingeniería Civil, A.A. 75267, Medellín, Colombia, yvalenc0@unal.edu.co*

Abstract

A parameter selection algorithm based on exhaustive search was used for the design of an optimal Tuned Mass Damper Inerter (TMDI), based on the classic tuned mass damper (TMD). The TMDI is a modified passive vibration control device, that combines the TMD with a mechanical flywheel element of negligible mass, called inerter, which is the mechanical equivalent of an electric capacitor that develops a resisting force proportional to the relative acceleration of its terminals. The optimal properties of the TMDI are determined using an exhaustive search methodology using a set of properties (mass, damping and stiffness) for the TMDI and evaluating the performance of the device by measuring the reduction of the structural response of the controlled system when it is seismically excited. Parameters as peak displacement, interstory drift and RMS value of displacement are stored and a new set of properties for the TMDI are selected, starting the process again. When all the possible combinations of properties are used, the algorithm compares the configuration of TMDI to determine which one is more efficient at reducing the peak displacement of the structure and the RMS value of the displacement, labeling it as the optimal configuration. To test the optimization methodology proposed, the performance of a TMDI used for the vibration control of a 11-story building is studied under seismic excitation by four different earthquake existing records. The results show that the proposed methodology is effective in finding the configuration to design an optimal TMDI.

Keywords: Tuned mass damper inerter; structural control; exhaustive search, optimization process.

2. Introduction

Research focused on passive vibration control of civil engineering structures has taken remarkable importance in countries subjected to significant seismic risk. Since its appearance [1], the Tuned Mass Damper (TMD) has become one of the most studied and tested control vibration device; however, considerable amounts of mass must be attached to the main structure to effectively reduced seismic performance of the TMD equipped structures, which in occasions may result impractical or economically unfeasible. Considering this, Marian and Giaralis [2] proposed the Tuned Mass Damper Inerter (TMDI), a novel device that couples the conventional TMD with the inerter [3], a device with negligible mass that induces an equivalent mass amplification effect called inertance, being a 1/200 ratio between the real device mass, and the inertance added [4]. In this novel mechanism, the inerter acts as a link between the TMD and the story floor immediately below the TMD location, in such a way that the large kinetic mass simulated by the inerter is used to improve the performance of the conventional TMD, and furthermore, decreasing its weight [5]. Subsequently, several authors contributed to the development of mathematical models and different configurations for TMDIs [6-8].

The accurate design of TMDI systems, as with TMDs, is based on finding the optimal tuning parameters that achieve the best performance of the system. Several authors [9-12] have contributed in this field through investigation of the response of single degree of freedom system, excited under harmonic or stochastic loads, where the optimization process objective is to minimize displacement or acceleration, or to maximize energy dissipation. The behavior of multi-degree of freedom systems equipped

with TMDIs was also investigated, alongside with the optimal design, based on parametric studies referred to the decrease in acceleration and displacement [13-15]. It is noteworthy, that in all these previous works, the numerical models employed to test the performance of TMDIs were only single degree of freedom systems or shear frame building structures; moreover, the dynamic action employed for the tuning processes is not compatible with the impulsive nature, and random frequencies that characterize the seismic action. Therefore, the effectiveness of TMDI systems has not been validated yet, for seismic approaches.

The investigation presented here, focuses on the optimal tuning parameters for TMDI systems computed through the use of an exhaustive-search based algorithm; the objective functions in the optimization process are based on strategic parameters that lead to an efficient design, such as horizontal peak displacement, interstory drift, and root mean square (RMS) values of horizontal displacements. The numerical model employed in the study is based on a 11-story building located in Medellin, Colombia, considering 11 horizontal degrees of freedom (one at each level) and applying a static condensation on the remaining vertical displacements and rotations degrees of freedom. This model is subjected to four different existing earthquake records. The results show that the proposed methodologies are effective in finding the configuration to design an optimal TMDI, achieving reductions of up to 30% in the story peak displacement and RMS value of the story displacement, and up to 25% in the maximum peak interstory drift.

2. Seismically excited multi-degree of freedom system equipped with tuned mass damper inerter (TMDI)

The inerter device (Fig.1) is a mechanical equivalent of the electric condenser [3]. This mechanism is an element of negligible mass with two nodes that can move independently from each other, generating a resisting force proportional to the relative accelerations of its two terminals, calculated according to equation. (1), where F is the resisting force on each node, b is the proportionality constant, in terms of mass, which defines the inerter device, and $\ddot{u}_i$ and $\ddot{u}_j$ son are the accelerations in nodes i and j, respectively:

$$F = b\left(\ddot{u}_i - \ddot{u}_j\right) \qquad (1)$$

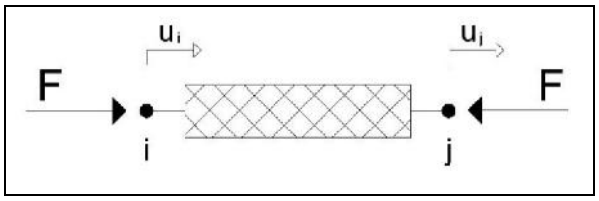

Fig. 1 – Inerter device idealization.

Equations of motion are laid out for the TMDI equipped n degrees of freedom structure represented in Fig.2. k_i, c_i and m_i symbolize the structure's stiffness, damping, and mass at each story i, respectively. The TMDI device is idealized as the combination of a conventional TMD and an inerter, where the constant b is the TMDI *inertance*, m_{TMDI} is its mass, while the ¿ stiffness and damping coefficients are k_{TMDI} y c_{TMDI}, respectively.

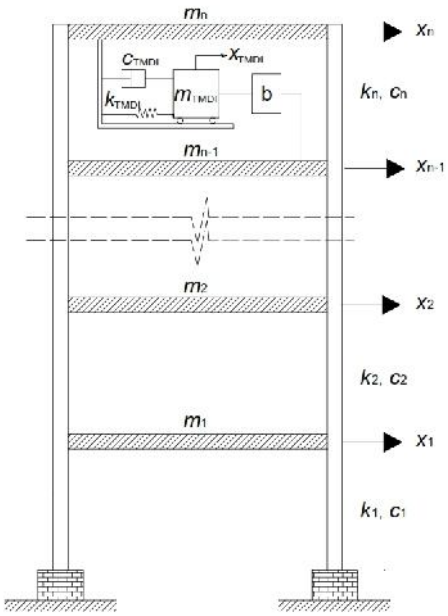

Fig. 2 – TMDI equipped *n* degrees of freedom system.

Thus, the dynamic behavior of the TMDI equipped n+1 degrees of freedom system, subjected to ground acceleration, may be modelled through the space-state representation stated with equation 2, where $\dot{\mathbf{z}}(t)$ represents the state vector first derivative, **A** is the transition state matrix, **B** is a matrix representing the location of the external excitation on the structural system, **M** is the system's mass matrix, **1** is a unitary vector of order (n+1), $\ddot{x}_g(t)$ is the time dependent soil acceleration, and **C** and **K** are is the system's damping and stiffness matrices, respectively, as shown below:

$$\dot{\mathbf{z}}(t) = \mathbf{A}\mathbf{z}(t) - \mathbf{B}\mathbf{M}\mathbf{1}\ddot{x}_g(t) \qquad (2)$$

$$\mathbf{z}(t) = \begin{Bmatrix} \dot{\mathbf{x}}(t) \\ \ddot{\mathbf{x}}(t) \end{Bmatrix}, \quad \mathbf{A} = \begin{bmatrix} \mathbf{0} & \mathbf{I} \\ -\mathbf{M}^{-1}\mathbf{K} & -\mathbf{M}^{-1}\mathbf{C} \end{bmatrix}, \quad \mathbf{B} = \begin{bmatrix} \mathbf{0} \\ \mathbf{M}^{-1} \end{bmatrix}, \quad \mathbf{M} = \begin{bmatrix} m_1 & 0 & 0 & 0 & \cdots & \cdots & 0 \\ 0 & m_2 & 0 & 0 & \cdots & \cdots & 0 \\ 0 & 0 & m_3 & 0 & \cdots & \cdots & 0 \\ \vdots & \vdots & \vdots & \ddots & \cdots & \cdots & \vdots \\ \vdots & \vdots & \vdots & \vdots & m_{n-1}+b & 0 & -b \\ \vdots & \vdots & \vdots & \vdots & 0 & m_n & 0 \\ 0 & 0 & \cdots & \cdots & -b & 0 & m_{TMDI}+b \end{bmatrix}$$

$$\mathbf{C} = \begin{bmatrix} c_1+c_2 & -c_2 & 0 & 0 & \cdots & \cdots & 0 \\ -c_2 & c_2+c_3 & -c_3 & 0 & \cdots & \cdots & 0 \\ 0 & -c_3 & c_3+c_4 & -c_4 & \cdots & \cdots & 0 \\ \vdots & \vdots & \vdots & \ddots & \cdots & \cdots & \vdots \\ \vdots & \vdots & \vdots & -c_{n-1} & c_{n-1}+c_n & -c_n & 0 \\ \vdots & \vdots & \vdots & 0 & -c_n & c_n+c_{TMDI} & -c_{TMDI} \\ 0 & 0 & \cdots & 0 & 0 & -c_{TMDI} & c_{TMDI} \end{bmatrix}, \quad \mathbf{K} = \begin{bmatrix} k_1+k_2 & -k_2 & 0 & 0 & \cdots & \cdots & 0 \\ -k_2 & k_2+k_3 & -k_3 & 0 & \cdots & \cdots & 0 \\ 0 & -k_3 & k_3+k_4 & -k_4 & \cdots & \cdots & 0 \\ \vdots & \vdots & \vdots & \ddots & \cdots & \cdots & \vdots \\ \vdots & \vdots & \vdots & -k_{n-1} & k_{n-1}+k_n & -k_n & 0 \\ \vdots & \vdots & \vdots & 0 & -k_n & k_n+k_{TMDI} & -k_{TMDI} \\ 0 & 0 & \cdots & 0 & 0 & -k_{TMDI} & k_{TMDI} \end{bmatrix}$$

3. TMDI optimal parameters selection methodology

This work utilizes an exhaustive-search optimization process, which is a simple and direct methodology resulting in accurate solutions, at the expense of a high processing power, and consisting in the examination of all possible solutions, continuously comparing which of these combinations afford the most efficient solution to the problem at the lowest cost.

Thus, the TMDI devices optimal design consists in the determination of the values for critical damping ratio, ζ_{TMDI}, defined with equation 3, and frequency ratio, υ_{TMDI}), defined with equation 4, for the dissipating device, where c_{TMDI}, m_{TMDI}, ω_{TMDI}, b and ω_1 are the TMDI's damping, mass, angular frequency, inertance and fundamental natural frequency, respectively:

$$\zeta_{TMDI} = \frac{c_{TMDI}}{2\left(m_{TMDI} + b\right)\mu_{TMDI}} \tag{3}$$

$$\upsilon_{TMDI} = \frac{\mu_{TMDI}}{\mu_1} \tag{4}$$

The proposed methodology starts with continuous closed sets of possible optimal parameter values for ζ_{TMDI} and υ_{TMDI}. First, the process generates a division of these sets in a finite number of values, encompassing all the optimal values set for each parameter. The optimization method utilizes all possible finite values combinations generated in the division process of the closed sets, in such a manner that each one of the discrete values, and its respective combination, are employed for the calculation of the TMDI's mass (m_{TMDI}), damping (c_{TMDI}) and stiffness (k_{TMDI}), based on expressions (3) and (4), assuming a fixed device mass ratio (μ) and a fixed inertance ratio (β) for the complete optimization process, where μ and β are defined with equations (5) and (6), where m_{TMDI}, m_1 y b are the TMDI mass, the generalized system mass, through which the structural system's fundamental natural frequency may be obtained, and the device's inertance value, respectively:

$$\mu = \frac{m_{TMDI}}{m_1} \tag{5}$$

$$\beta = \frac{b}{m_1} \tag{6}$$

Once the TMDI parameters are determined, the controlled structural system's response is calculated for each specific acceleration record. The response data is stored in a data base and the performance parameters are processed in order to stablish comparison criteria among the different examined value sets. In the next step, new discrete values are selected for ζ_{TMDI} and υ_{TMDI}, and the process is repeated. When the algorithm has exhausted all possible solutions to the optimization problem, the structure's maximum peak displacement, the root mean square (RMS) displacement values, and the peak story drift minimum values are defined, using equation 7 through 9.

$$OA1 = \min\left(\max\left(\left|X_{i\,peak}\right|\right)\right) \tag{7}$$

$$OA2 = \min\left(\max\left(\left|RMS\left(X_{ipeak}\right)\right|\right)\right) \tag{8}$$

$$OA3 = \min\left(\max\left(\left|\Delta_{ipeak}\right|\right)\right) \tag{9}$$

4. Case-study building

The proposed optimization technic is applied on a numeric model based on an existing 11-story reinforced concrete building located in Medellin, Colombia, shown in Fig.3 (a), which houses the city's official lottery. The structure is a combined frame and wall system, with story height of 2.72 m, as shown in Fig.3 (b). To simplify the dynamic analysis, one of the structure's planes was selected to model the optimization process, as shown in Fig.3 (c). The plane frame was idealized assuming infinitely

rigid floor diaphragms, so the horizontal degrees of freedom in each floor could be reduced to one, eliminating the vertical degrees of freedom, and condensing the rotational degrees of freedom. Thus, the model was reduced to one degree of freedom per story.

a) Building's frontal façade

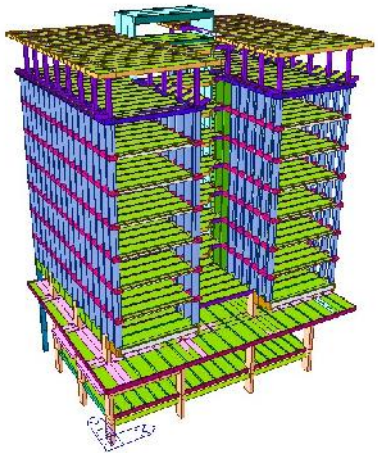

b) 3D structural model

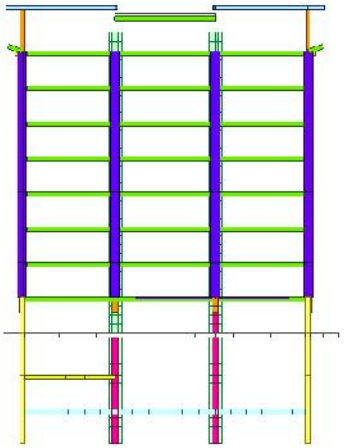

c) Plane frame to model the proposed method

Fig. 3 – Medellin's Lottery building.

Equations 10 and 11 show the stiffness and mass matrix for the model, respectively. The model's damping matrix (**C**) is assumed to be Rayleigh damping matrix, linearly proportional to the stiffness and mass, with a critical damping ratio of 5% for all modes.

$$\mathbf{K} = \begin{bmatrix} 311765 & -172446 & 48350.9 & -13110.7 & 2932 & -658.4 & 148.5 & -33.6 & 7.6 & -1.7 & 0.3 \\ & 195016 & -116165 & 44693.4 & -9953.8 & 2225.3 & -499.5 & 112.6 & -25.4 & 5.6 & -0.9 \\ & & 183933 & -148834 & 52580 & -11700.6 & 2613.6 & -586.1 & 131.7 & -28.7 & 4.6 \\ & & & 231499 & -162559 & 55631 & -12381.3 & 2765.8 & -619.2 & 134.4 & -21.4 \\ & & & & 235389 & -163428 & 55825.5 & -12424 & 2770.6 & -599.1 & 95.2 \\ & & & & & 235584 & -163470 & 55830.3 & -12403.9 & 2673 & -424.1 \\ & & \textit{SYMMETRIC} & & & & 235589 & -163450 & 55732.7 & -11971.7 & 1896.5 \\ & & & & & & & 235491 & -163018 & 53819 & -8513.8 \\ & & & & & & & & 233577 & -154509 & 38358 \\ & & & & & & & & & 195586 & -85108 \\ & & & & & & & & & & 53714 \end{bmatrix} \frac{KN}{m} \quad (10)$$

$$\mathbf{M} = \begin{bmatrix} 77.28 & 0 & 0 & 0 & 0 & 0 & 0 & 0 & 0 & 0 & 0 \\ & 77.94 & 0 & 0 & 0 & 0 & 0 & 0 & 0 & 0 & 0 \\ & & 78.02 & 0 & 0 & 0 & 0 & 0 & 0 & 0 & 0 \\ & & & 77.44 & 0 & 0 & 0 & 0 & 0 & 0 & 0 \\ & & & & 77.44 & 0 & 0 & 0 & 0 & 0 & 0 \\ & & & & & 77.44 & 0 & 0 & 0 & 0 & 0 \\ & & & & & & 77.44 & 0 & 0 & 0 & 0 \\ & & & \textit{SYMMETRIC} & & & & 77.44 & 0 & 0 & 0 \\ & & & & & & & & 77.44 & 0 & 0 \\ & & & & & & & & & 77.44 & 0 \\ & & & & & & & & & & 74.70 \end{bmatrix} Mg \quad (11)$$

Fixed values for mass ratio (μ) and inertance ratio (β) of 5% are used for the whole TMDI parameters selection process. Two closed value sets for parameters ζ_{TMDI}, and υ_{TMDI} are defined with equations 11 and 12:

$$0 \leq \zeta_{TMDI} \leq 0.5 \quad (11)$$

$$0 \leq \upsilon_{TMDI} \leq 2 \quad (12)$$

These ranges are typical for conventional TMDI devices and are a reasonable starting point for the TMDI parameters selection process [10]. The model is subjected to the earthquake records shown in Table 1.

Table 1 – Earthquake ground-motions records used in the optimization process.

Earthquake acceleration record	**Date**	**Magnitude**	**Peak acceleration (m/s^2)**	***RMS* value of acceleration (m/s^2)**
El Centro	May 18, 1940	6.9 M_W	3.1266	0.6005
Algarrobo	March 3, 1985	8.0 M_W	6.2885	1.4917
Kobe	January 17, 1995	6.9 M_W	8.0545	1.0443
Christchurch	February 22, 2011	6.2 M_W	8.0614	0.7318

The proposed method is applied to the model, calculating the main structure's response parameters in each step, as described above. The optimization process will be applied for *OA1, OA2 and OA3* indexes. Thus, a comparative analysis of the TMDI equipped model's performance is conducted. Table 2 shows TMDI design parameters ζ and υ, obtained in each of the three index alternatives, for β and μ fixed values of 5%.

Table 2 – TMDI optimization parameters for the different alternatives with β and μ of 5%

	El centro		Christchurch		Kobe		Algarrobo		Average value	
Optimization alternative	ζ_{TMDI}	υ_{TMDI}	ζ_{TMDI}	υ_{TMDI}	ζ_{TMDI}	υ_{TMDI}	ζ_{TMDI}	υ_{TMDI}	ζ_{TMDI}	υ_{TMDI}
OA1	0	0.02	0	0.02	0	0.10	0.01	0.02	0	0.04
OA2	0.14	0.02	0.09	0.02	0.17	0.02	0.07	0.02	0.12	0.02
OA3	0.29	0.03	0	0.02	0.08	0.14	0	0.08	0.09	0.07

Both damping and frequency ratios show optimization parameters that vary for each particular case, with the exception of the results for the *OA2* optimization index alternative, where the frequency ratio parameter results in a constant 2% for all earthquake ground motion records. For the peak displacement reduction optimization alternative, the best results are obtained with no damping (critical damping ratio value of 0%); For the peak displacement *RMS* reduction optimization alternative, the best results are obtained with a critical damping ratio value of around 12%, corresponding to the mean value of the performance under each of the four earthquake records. For both damping and frequency ratios, alternative *OA3* results in wider parameter variation between earthquake records, with average values of 9% and 7%, respectively. Fig.4 shows the TMDI design parameter distribution for each one of the three optimization alternatives used.

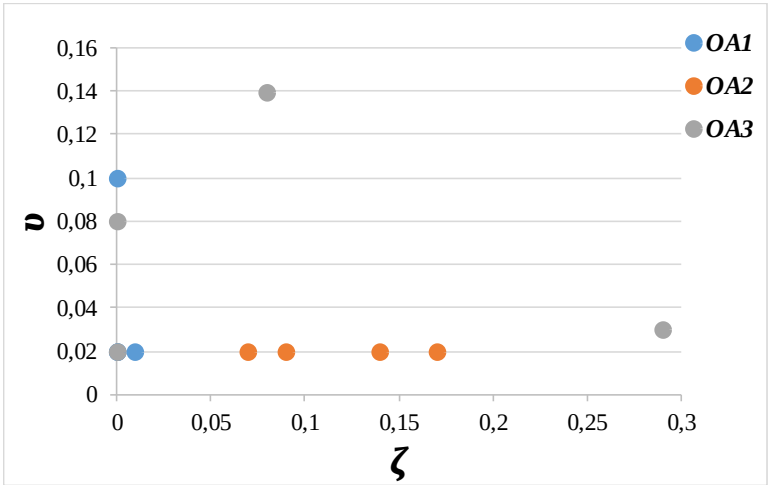

Fig. 4 – Design parameters distribution according to the optimization alternatives

Fig.5 shows the upper story displacement evolution against time, for the three alternative indexes of the TMDI equipped model, as compared with the model with no dissipation device, for each earthquake ground motion record.

Optimization alternative *OA1* generally results in the greatest response reduction for all four earthquake ground motions. Likewise, optimization alternative *OA3* presents the smallest displacement reductions, and in some cases results in displacement amplification, as compared with the model with no dissipation device.

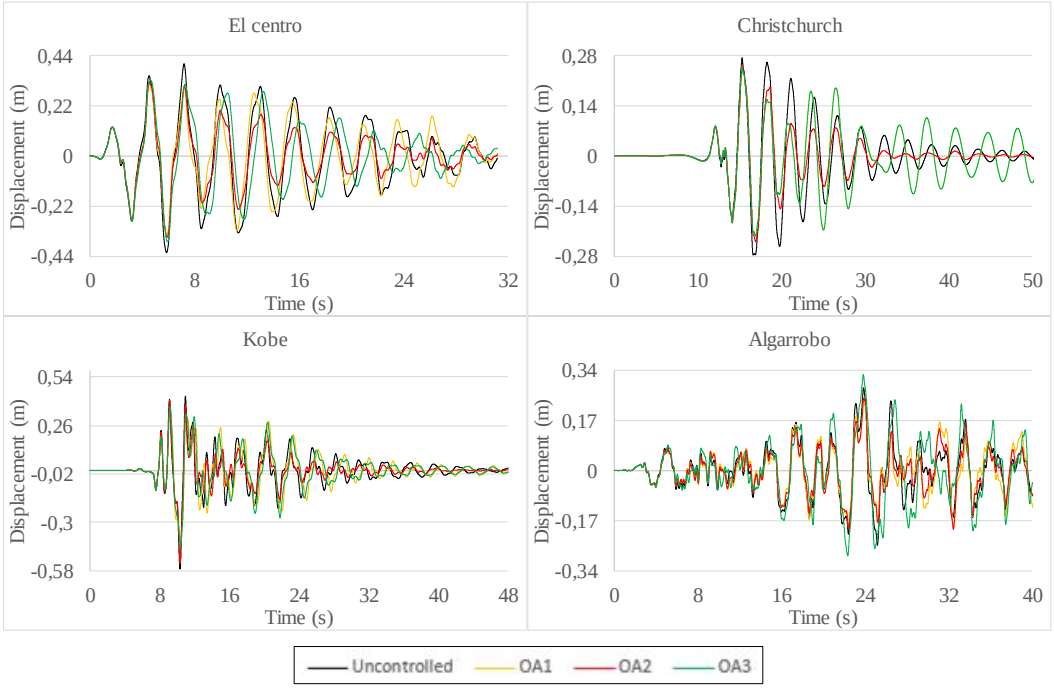

Fig. 5 – Displacement time history of the 11th story for the uncontrolled and controlled models under the four earthquake excitations used.

These results are corroborated reviewing the performance of some of the story response parameters of the TMDI equipped model, as shown in Fig.6.

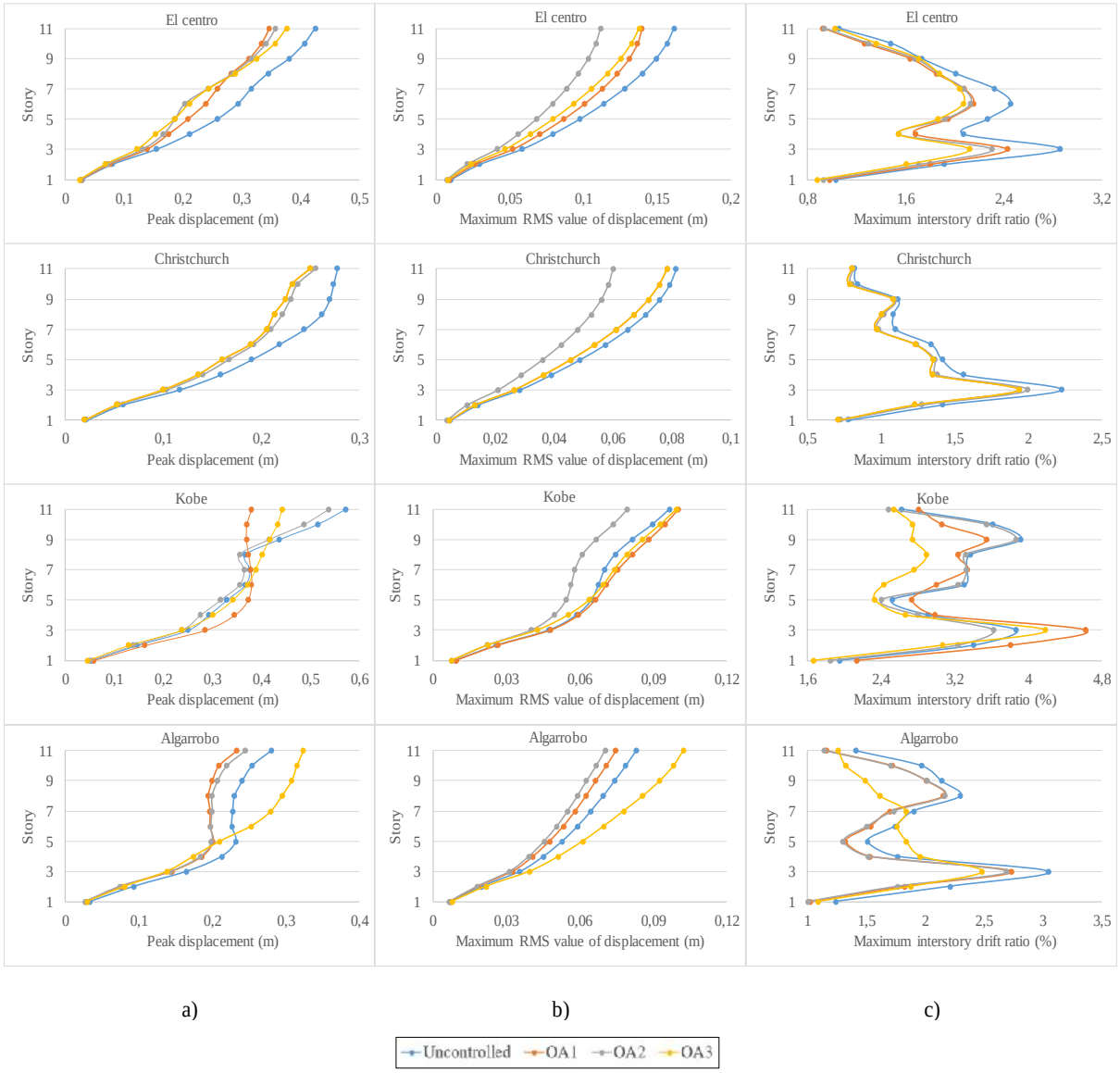

Fig. 6 – Uncontrolled and controlled story response parameters for the four different ground motion records used: a) Peak displacement, b) maximum RMS value of displacement, c) interstory drift ratio

Thus, it may be seen that TMDI devices designed using optimization alternative *OA2* are the most efficient, as it results in significant reductions, not only for the maximum displacement RMS value, but also for the story peak displacements and, for the most part, for the peak story drift. For example, for the model subjected to "El Centro" record, the TMDI designed with the *OA2* optimization alternative resulted in peak displacement reductions of up to 30.68% (at the sixth level), of up to 30.62% in peak displacement RMS value (at the upper level) and of up to 25.15% in the peak story drift (at the fourth story). The enhancement achieved with *OA2* in some cases exceeds the performance of the other optimization approaches, even in the response in which *OA1*, and *OA3* are focused. For example, when subjected to the "Algarrobo" ground motion, the peak displacement on the second floor is diminished by the TMDI by 16.96%, for the *OA1* alternative, while by the *OA2* alternative it is diminished by

19.80%, despite the fact that *OA2* is not focused on decreasing the peak displacement. The same also happens in some cases for the alternative in terms of de peak story drift. Thus, when subjected to the "Kobe" record, for the *OA2* alternative, the peak story drift ratio diminishes by 9.28%, while for the *OA3* alternative the reduction is limited to 4.39%. Table 3 shows a summary of response parameter reductions, associated to each floor's displacement.

Table 3 – Response reduction percentages for the different cases studied

	Story	**Peak displacement reduction (%)**			**RMS value of the story displacement reduction (%)**			**Peak interstory drift ratio reduction (%)**		
		OA1	*OA2*	*OA3*	*OA1*	*OA2*	*OA3*	*OA1*	*OA2*	*OA3*
El Centro	*1*	4,50	9,49	14,35	11,36	28,41	21,29	4,51	9,49	14,64
	2	5,56	10,29	15,70	9,51	27,28	19,14	5,95	10,58	15,94
	3	10,67	15,04	21,33	10,73	28,79	19,46	14,15	18,58	25,08
	4	16,90	20,88	27,18	11,00	29,43	19,02	18,48	25,15	25,11
	5	19,25	27,78	27,93	10,84	29,68	18,10	13,09	14,33	16,78
	6	18,72	30,68	28,09	10,96	30,02	17,40	11,28	12,28	14,67
	7	18,19	23,31	22,81	11,19	30,27	16,77	10,28	10,56	11,96
	8	17,88	17,26	16,02	11,52	30,43	16,20	6,87	5,83	5,48
	9	17,94	16,86	14,41	12,02	30,56	15,72	5,28	3,14	1,22
	10	17,89	15,86	12,04	12,35	30,41	14,86	14,06	11,74	7,36
	11	18,41	15,87	11,36	13,23	30,62	14,25	10,13	9,04	0,22
Christchurch	*1*	8,29	5,91	8,29	11,50	28,55	11,50	8,29	5,91	8,29
	2	9,21	6,02	9,21	6,03	24,67	6,03	12,08	8,51	12,08
	3	14,19	11,04	14,19	5,75	24,88	5,75	12,23	9,53	12,23
	4	14,45	11,30	14,45	6,50	25,73	6,50	12,41	10,59	12,41
	5	15,76	12,31	15,76	4,90	24,72	4,90	3,06	2,20	3,06
	6	13,42	11,71	13,42	5,40	25,38	5,40	6,59	6,41	6,59
	7	15,51	13,68	15,51	5,89	26,06	5,89	8,85	7,96	8,85
	8	18,37	15,11	18,37	5,23	25,89	5,23	5,97	4,50	5,97
	9	16,53	14,60	16,53	3,73	25,12	3,73	1,82	1,12	1,82
	10	15,30	13,26	15,30	3,91	25,81	3,91	2,54	0,66	2,54
	11	9,89	7,95	9,89	3,10	25,89	3,10	0,96	-0,26	0,96
Kobe	*1*	-9,64	4,91	14,43	-5,18	12,79	14,57	-9,64	4,91	14,43
	2	-11,43	4,58	11,24	-2,44	14,78	13,93	-12,57	4,39	9,28
	3	-14,34	4,83	4,75	-2,22	14,75	9,30	-19,91	6,03	-8,49
	4	-18,33	5,58	-3,19	-2,68	14,66	4,65	-2,78	3,48	8,32
	5	-13,38	3,70	-3,99	-3,58	15,12	0,06	-9,25	3,94	6,83
	6	-3,59	3,12	-1,13	-5,74	15,82	-3,92	8,31	0,98	25,76
	7	-0,70	2,94	-3,40	-7,89	17,22	-5,87	-0,81	-0,67	16,61
	8	-1,88	3,17	-9,49	-9,97	17,58	-7,04	3,28	0,75	13,48
	9	15,24	4,63	4,27	-8,83	17,84	-5,81	8,98	0,70	29,67
	10	27,92	5,33	15,75	-6,36	17,42	-4,40	14,95	1,57	23,91
	11	33,47	5,92	22,37	-4,36	17,38	-3,58	-7,70	4,88	2,74
Algarrobo	*1*	15,36	17,13	9,89	-0,81	2,89	-14,46	15,36	17,13	9,89
	2	16,96	19,80	13,11	6,05	9,63	-9,30	17,21	19,98	14,73
	3	12,37	13,56	16,30	6,83	10,60	-13,01	9,39	10,70	17,64
	4	12,17	13,28	17,78	8,98	12,90	-14,09	13,30	14,05	-11,07
	5	13,10	13,95	9,05	8,43	12,68	-17,70	12,26	13,62	-21,96
	6	12,90	12,66	-11,85	9,69	14,19	-18,37	11,02	12,82	-1,96
	7	13,32	12,27	-23,20	9,17	13,98	-21,77	9,10	7,50	1,95
	8	15,44	13,37	-28,07	9,55	14,57	-24,19	5,44	5,01	29,18
	9	16,77	13,82	-28,15	10,14	15,25	-25,15	5,59	5,36	30,03
	10	17,66	13,70	-23,97	9,32	14,53	-25,92	11,56	12,26	32,00
	11	16,64	12,60	-15,68	8,96	14,24	-24,68	16,92	17,98	9,67

Conclusions

TMDI devices were designed in the present work, for the vibration control of a building subjected to various earthquake records. The design parameters were optimized with an exhaustive-search based process. Three objective functions were explored in order to reduce the structural response of the TMDI equipped model. Results show that all three optimization alternatives studied effectively reduce, in a smaller or greater degree, the response records of the controlled building. A comparative analysis of the response parameters indicates that the TMDI designed with the optimization alternative which aims to minimize the structure's peak displacement RMS, produces the most balanced, stable and successful control mechanisms ofr the reduction of the different response parameters evaluated, diminishing peak displacements and peak story displacement RMS values in between 3 % and 30%, and story drift ratios in up to 25%. Thus, the proposed methodology proved to be valuable and of simple and straightforward implementation, and may be used when designing a TMDI equipped project.

Acknowledgements

The authors are grateful for the support provided by the Universidad Nacional de Colombia – Sede Medellín for the development of this work.

References

[1] Frahm H (1911) Device for damping vibrations of bodies. U.S. Pat. No 989,958. https://doi.org/10.1016/j.tree.2005.10.010.
[2] Marian L, Giaralis A (2013) Optimal design of inerter devices combined with TMDs for vibration control of buildings exposed to stochastic seismic excitations. Safety, Reliability, Risk and Life-Cycle Performance of Structures and Infrastructures-Proceedings of the 11th International Conference on Structural Safety and Reliability, ICOSSAR 2013 (pp. 1025-1032). CRC Press.
[3] Smith MC (2002) Synthesis of mechanical networks: The inerter. IEEE Transactions on automatic control, 47(10), 1648-1662. https://doi.org/10.1109/TAC.2002.803532.
[4] Papageorgiou C, Smith MC (2005) Laboratory Experimental Testing of Inerters. Proceedings of the 44th IEEE Conference on Decision and Control (pp. 3351-3356). IEEE. https://doi.org/10.1109/CDC.2005.1582679.
[5] Giaralis A, Marian L (2016) Use of inerter devices for weight reduction of tuned mass-dampers for seismic protection of multi-story building: The Tuned Mass-Damper-Interter (TMDI). Active and Passive Smart Structures and Integrated Systems (Vol. 9799, p. 97991G). International Society for Optics and Photonics. https://doi.org/10.1117/12.2219324.
[6] Salvi J, Giaralis A (2016) Concept study of a novel energy harvesting-enabled tuned mass-damper-inerter (EH-TMDI) device for vibration control of harmonically-excited structures. Journal of Physics: Conference Series (Vol. 744, No. 1, p. 012082). IOP Publishing. https://doi.org/10.1088/1742-6596/744/1/012082.
[7] Javidialesaadi A, Wierschem N (2017) Seismic Performance Evaluation of Inerter-Based Tuned Mass Dampers Dampers. 3RD Huixian International Forum on Earthquake Engineering for Young Researchers, University of Illinois, Urbana-Champaign, IL.
[8] Lazarek M, Brzeski P, Perlikowski P (2018) Design and identification of parameters of tuned mass damper with inerter which enables changes of inertance, Mechanism and Machine Theory, 119, 161-173. https://doi.org/10.1016/j.mechmachtheory.2017.09.004.
[9] Marian L, Giaralis A (2015) Optimal design of a novel tuned mass-damper-inerter (TMDI) passive vibration control configuration for stochastically support-excited structural systems. Probabilistic Engineering Mechanics, 38, 156-164. 38 156–164. https://doi.org/10.1016/j.probengmech.2014.03.007.
[10] Marian L (2016) The tuned mass damper inerter for passive vibration control and energy harvesting in dynamically excited structural systems.
[11] Marian L, Giaralis A (2017) The tuned mass-damper-inerter for harmonic vibrations suppression, attached mass reduction, and energy harvesting. Smart structures and systems, 19(6), 665-678. https://doi.org/10.12989/sss.2017.19.6.665.
[12] Pietrosanti D, De Angelis M, Basili M (2017) Optimal design and performance evaluation of systems with Tuned Mass Damper Inerter (TMDI). Earthquake Engineering & Structural Dynamics, 46(8), 1367-1388. https://doi.org/10.1002/eqe.2861.
[13] Giaralis A, Taflanidis AA (2015) Reliability-based Design of Tuned Mass-Damper-Inerter (TMDI) Equipped Multi-storey Frame Buildings under Seismic Excitation. 2th International Conference on Applications of Statistics and Probability in Civil Engineering, ICASP. University of British Columbia Library.

[14] Giaralis A, Taflanidis AA (2018) Optimal tuned mass-damper-inerter (TMDI) design for seismically excited MDOF structures with model uncertainties based on reliability criteria. Structural Control and Health Monitoring, 25(2), e2082. 1–22. https://doi.org/10.1002/stc.2082.

[15] Ruiz R, Taflanidis AA, Giaralis A, Lopez-Garcia D (2018) Risk-informed optimization of the tuned mass-damper-inerter (TMDI) for the seismic protection of multi-storey building structures. Engineering Structures, 177, 836-850. https://doi.org/10.1016/j.engstruct.2018.08.074.

